Global and Planetary Change 195 (2020) 103352

Contents lists available at ScienceDirect

Global and Planetary Change

journal homepage: www.elsevier.com/locate/gloplacha

Ocean-atmosphere interactions over the western South Atlantic during Heinrich stadials

I.M. Venancio [a,b,f,*], M.H. Shimizu [a], T.P. Santos [b], D.O. Lessa [b], B.B. Dias [b], C.M. Chiessi [c], S. Mulitza [d], H. Kuhnert [d], R. Tiedemann [e], M. Vahlenkamp [d], T. Bickert [d], A.L. Belem [f], G. Sampaio [a], A.L.S. Albuquerque [b], C. Nobre [g]

[a] Center for Weather Forecasting and Climate Studies (CPTEC), National Institute for Space Research (INPE), Cachoeira Paulista, Brazil
[b] Programa de Geociências (Geoquímica), Universidade Federal Fluminense, Niterói, Brazil
[c] School of Arts, Sciences and Humanities, University of São Paulo, São Paulo, Brazil
[d] MARUM-Center for Marine Environmental Sciences, University of Bremen, Bremen, Germany
[e] Alfred Wegener Institute for Polar and Marine Research, Bremerhaven, Germany
[f] Programa de Pós-Graduação Dinâmica dos Oceanos e da Terra, Universidade Federal Fluminense, Niterói, Brazil
[g] Institute for Advanced Studies, University of São Paulo, São Paulo, Brazil

A B S T R A C T

Slowdowns of the Atlantic meridional overturning circulation during Heinrich stadials (HS) caused reductions in cross-equatorial heat transport, southward shifts of the Intertropical Convergence Zone and intensification of precipitation over eastern tropical South America. While these changes are well described, the associated spatial sea surface temperature (SST) patterns are still unclear. Here, we analyze proxy data to assess changes in ocean-atmosphere interactions during HS over the western South Atlantic. Our SST proxy records show contrasting patterns between the tropical (warming) and the subtropical (no change) western South Atlantic during HS. We propose that the distinct SST behavior in the subtropics was associated with the cloud cover effect of the South Atlantic Convergence Zone over the upper ocean.

1. Introduction

The slowdown of the Atlantic meridional overturning circulation (AMOC) during Heinrich stadials (HS) (McManus et al., 2004; Böhm et al., 2015; Henry et al., 2016) caused a reduction in cross-equatorial heat transport, which in turn resulted in a cooling of the Northern Hemisphere and a warming of the Southern Hemisphere, as described by the thermal bipolar seesaw (Broecker, 1998; Stocker and Johnsen, 2003). This asymmetric temperature response causes a southward displacement of the Intertropical Convergence Zone (ITCZ) (Mulitza et al., 2017; Zhang et al., 2017) and strengthens precipitation over eastern tropical South America across at least part of the region influenced by the South Atlantic Convergence Zone (SACZ) (Fig. 1; Stríkis et al., 2018; Campos et al., 2019). Although such changes are well described and supported by proxy data, regional ocean-atmosphere feedbacks over the western South Atlantic have not yet been fully explored. Understanding ocean-atmosphere feedbacks during periods of fluctuations in AMOC strength (Arz et al., 1998; Mulitza et al., 2017) becomes crucial even if a debate still exists whether the AMOC is stable (Parker, 2016) or weakening in recent decades (Caesar et al., 2018). Recent studies point to a serious bias in the modeled AMOC stability, in favoring a stable AMOC and overlooking an AMOC collapse in climate projections (Drijfhout et al., 2011; Liu et al., 2017).

During HS1, western Atlantic sea surface temperatures (SST) in the Brazil Current (BC) and the North Brazil Current (NBC) (Fig. 1) were in phase on millennial scales (Weldeab et al., 2006; Chiessi et al., 2015). However, Chiessi et al. (2015) observed that the NBC domain showed larger SST increases than the BC, suggesting regional differences in SST changes during HS. Interestingly, sites located between 20°S and 30°S in the South Atlantic lacked a significant SST response in the BC domain during HS (Carlson et al., 2008; da Portilho-Ramos et al., 2015; Santos et al., 2017; Pereira et al., 2018).

Recent evidence points towards a widespread increase in precipitation over eastern South America partially over the region occupied by the SACZ during HS (Stríkis et al., 2015; Stríkis et al., 2018; Campos et al., 2019). Ocean models and observational data show that an intensification of SACZ (hence increased cloud cover) under modern conditions reduces incident shortwave solar radiation, which cools the

* Corresponding author at: Center for Weather Forecasting and Climate Studies (CPTEC), National Institute for Space Research (INPE), Cachoeira Paulista, Brazil.
E-mail address: igor.venancio@inpe.br (I.M. Venancio).

https://doi.org/10.1016/j.gloplacha.2020.103352
Received 12 June 2020; Received in revised form 18 September 2020; Accepted 14 October 2020
Available online 17 October 2020

underlying ocean in the subtropics. This in turn can weaken pre-existing positive SST anomalies (Chaves and Nobre, 2004; De Almeida et al., 2007; Nobre et al., 2012). The South Equatorial Current (SEC) feeds the BC and, on seasonal timescales, latitudinal migrations of the bifurcation are coupled to ITCZ displacements (Rodrigues et al., 2007), with the SEC bifurcation moving northward simultaneously with a southward ITCZ displacement. Accordingly, southward ITCZ migrations reported for HS (Wang et al., 2004; Jennerjahn et al., 2004; Mulitza et al., 2017) were probably followed by northward migrations of the SEC bifurcation (Venancio et al., 2018). This would enhance the transport of warm waters to the BC and increase SST at the subtropical South Atlantic. These regional ocean-atmosphere feedback mechanisms need to be considered when interpreting paleotemperature records from the western South Atlantic on millennial timescales.

We investigate the occurrence of ocean-atmosphere interactions during HS in the western South Atlantic. We show new high-resolution SST records derived from planktonic foraminiferal Mg/Ca from the western equatorial Atlantic and compare these new results with published SST records from the subtropical South Atlantic over the past 70 ka. Our results reveal distinct SST patterns between the tropical and the subtropical South Atlantic due to the influence of regional ocean-atmosphere feedbacks during HS (i.e. SACZ-SST feedback).

2. Study area

Marine sediment cores GL-1248 (0.55°S, 43.24°W, 2264 m water depth) (Venancio et al., 2018) and GeoB16202-2 (1°54.50′ S, 41°35.50′ W, 2248 m water depth) (Mulitza et al., 2013) were collected in the western equatorial Atlantic, off northeastern Brazil (Fig. 1). Here, the southward-flowing BC and the northward-flowing NBC originate from the bifurcation of the South Equatorial Current (SEC) at ~10°S and dominate the upper ocean circulation (Peterson and Stramma, 1991; Stramma and England, 1999). In the surface-ocean (<100 m), the BC and the NBC transport Tropical Water (TW), which is a warm (>20 °C) and saline (>36) water mass.

Off northeastern Brazil, seasonal changes in the trade wind system drive the variability of the NBC transport. During austral summer and fall, the ITCZ relocates southward, and the northeast (NE) trade winds strengthen (Hastenrath and Merle, 1987; Stramma et al., 1995). These shifts the SEC bifurcation northward and weakens the NBC (Rodrigues et al., 2007). At the same time rainfall over northeastern Brazil increases, peaking from March to April (Hastenrath, 2012).

Core sites located off southeastern Brazil are influenced by variations in the BC transport (Fig. S1). In this region, warm waters prevail during austral summer when BC transport reaches its maximum (Matano et al., 1993). The SST variations off southeastern Brazil affect precipitation over southeastern South America, where positive SST anomalies have been correlated with increased precipitation and an intensification of the SACZ (Chaves and Nobre, 2004).

3. Material and methods

The age model of core GL-1248 is based on twelve AMS radiocarbon ages and the alignment of the Ti/Ca record of core GL-1248 to the ice $\delta^{18}O$ record of the North Greenland Ice Core Project (NGRIP) using the extended Greenland Ice Core Chronology (GICC05modelext) (Table S1) (NGRIP members, 2004; Wolff et al., 2010). Details of the age model of core GL-1248 are found in Venancio et al. (2018). The age model for core GeoB16202-2 is based on 13 AMS radiocarbon ages (Table S1) and its full description is found in Mulitza et al. (2017). Downcore ages of core GeoB16202-2 were modeled using BACON software version 2.2 (Blaauw and Christen, 2019) and for core GL-1248 using the software clam 2.2 (Blaauw, 2010).

Both cores (GeoB16202-2 and GL-1248) were analyzed for Mg/Ca in

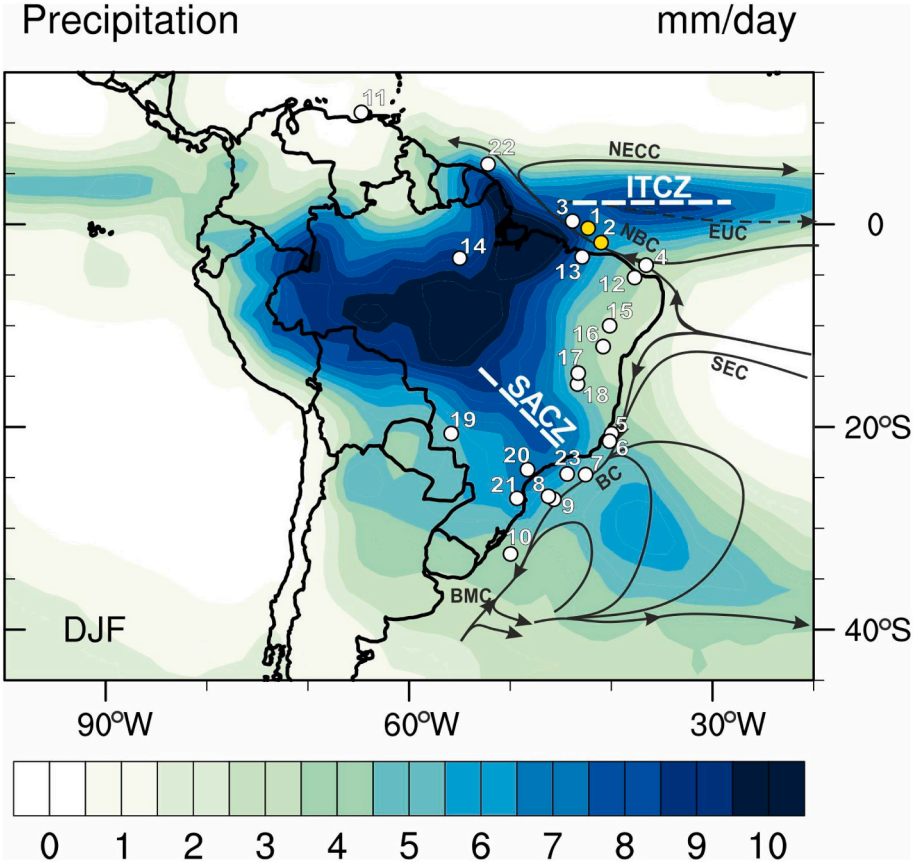

Fig. 1. Map showing the austral summer (December-January-February) precipitation (mm/day) in South America. Precipitation data extracted from the Climate Prediction Center (CPC) Merged Analysis of Precipitation (CMAP) (Xie and Arkin, 1997). White dashed lines indicate the main climatological features of the South America: South Atlantic Convergence Zone (SACZ) and Intertropical Convergence Zone (ITCZ). Black arrows show the main features of the upper ocean circulation: Brazil Current (BC), Brazil-Malvinas Confluence (BMC), Equatorial Undercurrent (EUC), North Brazil Current (NBC), North Equatorial Countercurrent (NECC) and South Equatorial Current (SEC). Yellow dots mark the location of our study sites (1- GL-1248, 2- GeoB16202-2). The white dots mark the location of other records discussed in the text (3- CDH-86, Nace et al., 2014; 4- GeoB3129-3911, Weldeab et al., 2006; 5- GL-75, da Portilho-Ramos et al., 2015; 6- GL-74, da Portilho-Ramos et al., 2015; 7- GL-1090, Santos et al., 2017; 8- GeoB2107-3, Pereira et al., 2018; 9- 36GGC, Carlson et al., 2008; 10- GeoB6211-2, Chiessi et al., 2015; 11- MD03-2621, Deplazes et al., 2013; 12- RN record, Cruz et al., 2009; 13- Caçó Lake, Sifeddine et al., 2003; 14- Paraíso Cave, Wang et al., 2017; 15- Toca da Boa Vista Cave, Wang et al., 2004; 16- Paixão/Marota Cave, Stríkis et al., 2015, 2018; 17- Lapa Grande Cave, Stríkis et al., 2018; 18- Lapa Sem Fim Cave, Stríkis et al., 2015, 2018; 19- Jaraguá Cave, Novello et al., 2017; 20- Santana Cave, Cruz et al., 2006; 21- Botuverá Cave, Cruz et al., 2005; 22- GeoB16224-1, Crivellari et al., 2018, 2019; 23- NAP 63–1, Dauner et al., 2019). (For interpretation of the references to colour in this figure legend, the reader is referred to the web version of this article.)

planktonic foraminifera *Globigerinoides ruber* (white). In the case of GL-1248, the upper 12.1 m (ca. 76 kyr) of the core were analyzed. For core GL-1248, Mg/Ca analyses were performed on samples comprising 30 shells of *G. ruber* (white, 250–300 μm), while for core GeoB16202-2, Mg/Ca analyses were performed on samples with 10–30 shells of *G. ruber* (white, 350–500 μm) (Vahlenkamp, 2013). The samples were gently crushed and cleaned following the procedure described by Barker et al. (2003). Before dilution, samples were centrifuged for 10 min to exclude any remaining insoluble particles from the analyses (Groeneveld and Chiessi, 2011). The diluted solutions of core GL-1248 were analyzed with an Agilent Technologies 700 Series ICP-OES equipped with a micro-nebulizer and coupled to an ASX-520 Cetac autosampler at MARUM. Mg/Ca values are averages from three replicate runs. After every five samples, one of two internal laboratory standards was measured to estimate the external reproducibility. Mean ± 1 standard deviation (SD) were 5.165 ± 0.024 mmol/mol for Mg/Ca for standard 1, and 3.294 ± 0.012 mmol/mol for Mg/Ca for standard 2. The samples from core GeoB16202-2 were analyzed on a ThermoFinnigan Element 2 Sector Field Inductively Coupled Plasma Mass Spectrometer (ICP-MS). Analytical errors of the elemental concentrations (standard deviations based on 10 runs) were better than 0.4%. For both cores, only samples with Al/Ca <0.5 μmol/mol were used in order to avoid contamination from clay minerals.

The Mg/Ca results were converted to temperatures using the Mg/Ca-temperature equation of Gray and Evans (2019) for *G. ruber* (white). This equation iteratively corrects for seawater salinity and carbonate chemistry effects and we followed the method that uses pCO_2 to estimate seawater pH (Gray and Evans, 2019). For the sake of consistency, we also applied the same equation for the Mg/Ca values of core GL-1090 (Santos et al., 2017), with which we will compare our results.

4. Results

The Mg/Ca values of *G. ruber* (white) converted to SST estimations for cores GL-1248 and GeoB16202-2 are shown in Fig. 2. For core GeoB16202-2, Mg/Ca values of *G. ruber* (white) varied from 3.29 mmol/mol to 5.22 mmol/mol, with a mean value of 4.07 mmol/mol. These values correspond to SSTs ranging between 23 °C and 29.7 °C, with a mean value of 25.7 °C. The top core SST estimate (26.9 °C) was similar to the modern annual SST for this site, which is 27.1 ± 0.4 °C (Locarnini et al., 2018; Fig. S1). SST increases (ca. 3–5 °C) were observed during the Younger Dryas (YD) and HS1. The lowest SST value (23 °C) occurred in the glacial period at 18.6 ka, prior to HS1. The mean 2σ error for the SST estimates from GeoB16202-2 was 1.5 °C.

For core GL-1248, Mg/Ca values of *G. ruber* (white) varied from 2.94 mmol/mol to 5.02 mmol/mol, with a mean value of 3.7 mmol/mol. The corresponding SSTs, range between 21.2 °C and 28.5 °C, with a mean value of 24.3 °C. The top core SST estimate (27.6 °C) was similar to the modern annual SST for this site, which is 27.5 ± 0.2 °C (Locarnini et al., 2018; Fig. S1). Major SST increases (ca. 4 °C) can be observed during HS6, HS4 and HS3, while moderate warmings (ca. 2–3 °C) are associated with HS5a, HS5 and the YD (Fig. 2). The lowest SST value (21.2 °C) occurred in the glacial period at 30.1 ka, prior to HS3. The mean 2σ error for the SST estimates from GL-1248 was also 1.5 °C.

5. Discussion

5.1. SST responses along the western Atlantic during Heinrich Stadials

Our data from cores GeoB16202-2 and GL-1248 show increasing SST during several HS and the YD (Fig. 2) as previously reported for the NBC domain (Weldeab et al., 2006; Crivellari et al., 2018, 2019). These SST increases reflect the accumulation of heat in the western equatorial Atlantic due to reduced cross-equatorial heat transport (Mix et al., 1986; Shakun et al., 2012) linked to AMOC slowdowns (McManus et al., 2004; Böhm et al., 2015; Henry et al., 2016). Local processes may contribute to this pattern of warm water accumulation in the western equatorial Atlantic. For example, weakening of the NBC and of the central branch of the SEC during HS (Weldeab et al., 2006; Venancio et al., 2018) due to less intensive southeast trade winds may enhance this stagnation of warm waters in the western equatorial Atlantic. Weakening of the southeast trade winds can occur in the absence of AMOC changes, for example due to low-latitude insolation changes (Venancio et al., 2018). Hence, changes in trade wind intensity and NBC strength are not exclusively related to the bipolar seesaw. During HS, if SST changes in the western equatorial South Atlantic were only a response to the bipolar

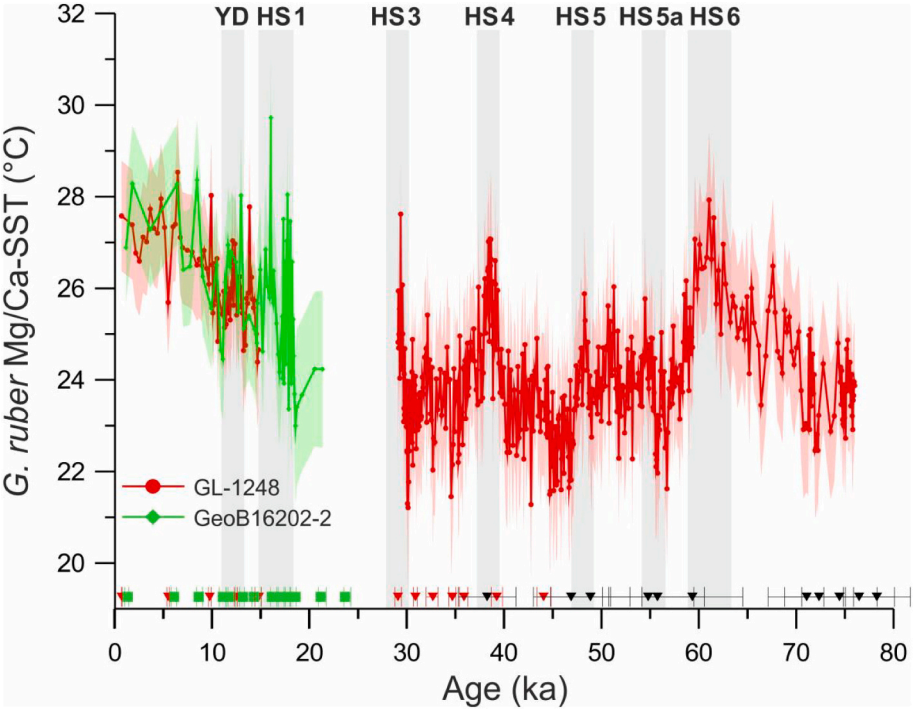

Fig. 2. Mg/Ca-sea surface temperature (SST) from cores GL-1248 (red line and dots) and GeoB16202-2 (green line and diamonds). SST was estimated using the equation from Gray and Evans (2019) and the 2σ error is represented by the envelopes of the curves. The grey bars highlight Heinrich stadials (HS) and the Younger Dryas (YD). Age control points for GL-1248 (radiocarbon dates – red; tie-points – black) and for GeoB16202-2 (radiocarbon dates – green) are shown with their respective uncertainties (2σ) close to the x-axis. Core GL-1248 presents a hiatus between 29 and 15 ka (Venancio et al., 2018). (For interpretation of the references to colour in this figure legend, the reader is referred to the web version of this article.)

seesaw, one could expect that the increase in SST due to heat accumulation should be proportional to the duration of the stadials (EPICA Community Members, 2006) and shall be relatively homogenous spatially, but this is not the case. Our data show that during HS5a and HS5 a minor increase in SST is observed compared to HS6, HS4, HS3 and HS1 (Fig. 2). Such minor increases in SST can be explained by shoaling of the seasonal thermocline (Venancio et al., 2018), where cold central waters closer to the surface partially dampen the surface warming. Despite the heterogeneous SST responses in terms of magnitude between different HS, warming was systematically recorded in the western equatorial Atlantic during these events.

Based on the high temporal resolution Mg/Ca SST records available by then, Chiessi et al. (2015) described an in-phase SST evolution between records from the southernmost BC and the central NBC domains during HS1 (Weldeab et al., 2006; Chiessi et al., 2015). New HS1 proxy records from the BC (Fig. 3c-d) and NBC (Fig. 3a-b), however, do not display similar SST variations (Carlson et al., 2008; Chiessi et al., 2015; Santos et al., 2017; Pereira et al., 2018; Dauner et al., 2019). Nevertheless, we must point out that some of the BC records have low temporal resolution for HS1 (i.e. da Portilho-Ramos et al., 2015) and others reconstruct the SST using the Modern Analog Technique (MAT) (i.e. da Portilho-Ramos et al., 2015; Pereira et al., 2018) or lipid-based biomarkers (i.e. Dauner et al., 2019), instead of Mg/Ca. The use of different SST proxies may partially explain the differences between SST records in the BC domain, especially in terms of mean SST values. However, the MAT has been commonly used to generate reliable SST records along the Brazilian coast (i.e. da Portilho-Ramos et al., 2015; Pereira et al., 2018; Lessa et al., 2017; Lessa et al., 2019). Only in Brazilian coastal upwelling

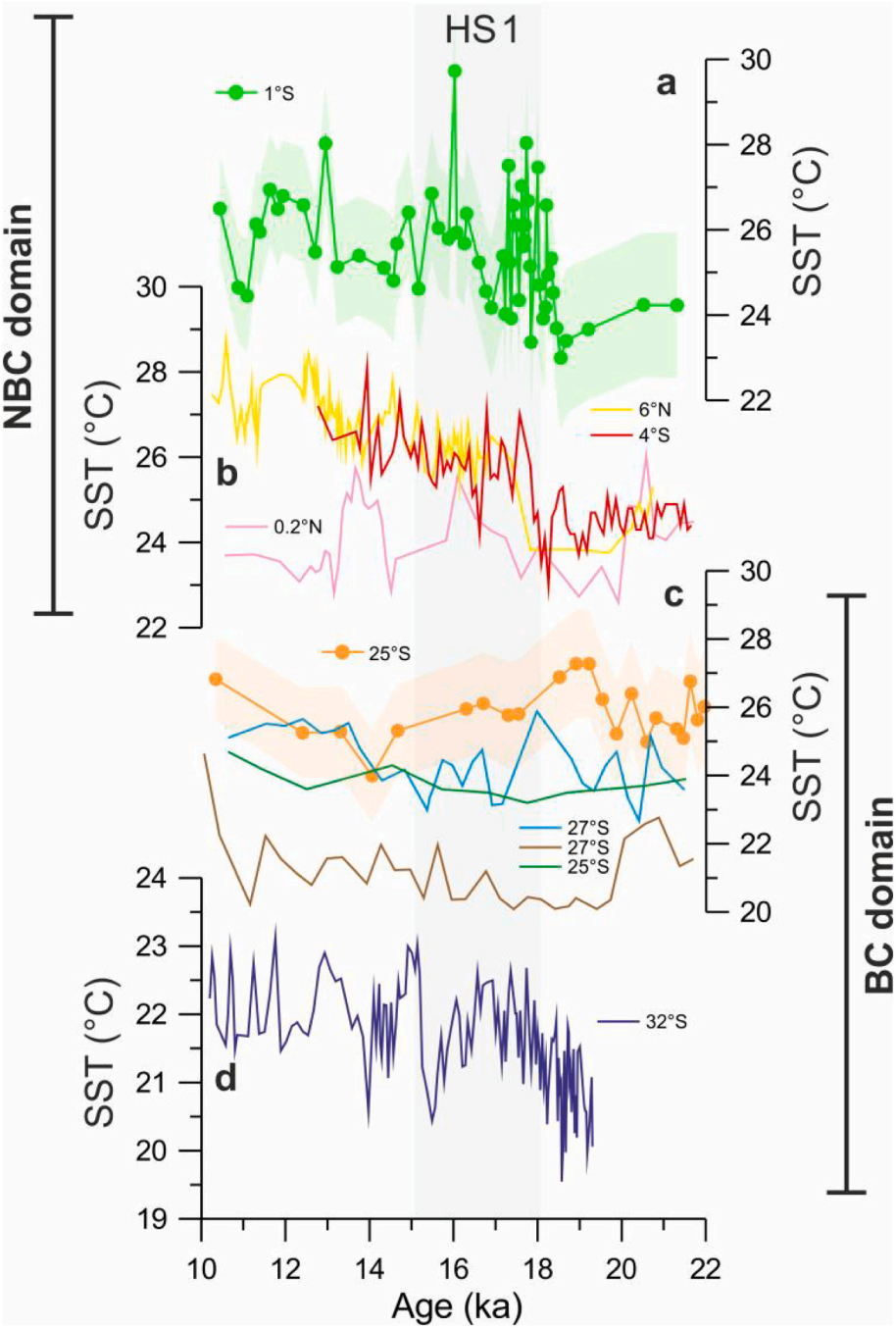

Fig. 3. Sea surface temperatures (SST) from the North Brazil Current (NBC) and Brazil Current (BC) domains. (a) Mg/Ca-SST derived from *Globigerinoides ruber* from core GeoB16202-2 (this study) (light green line and dots) with 2σ error envelope. (b) Other NBC domain SSTs: Mg/Ca-SST derived from *Globigerinoides ruber* from core GeoB3129 (Weldeab et al., 2006) (red line); Mg/Ca-SST derived from *Globigerinoides ruber* from core CDH-86 (Nace et al., 2014) (pink line); Mg/Ca-SST derived from *Globigerinoides ruber* from core GeoB16224-1 (Crivellari et al., 2018, 2019) (yellow lin). (c) BC domain SSTs: Mg/Ca-SST derived from *Globigerinoides ruber* from core GL-1090 (Santos et al., 2017) (orange line and dots) with 2σ error envelope; Temperature at 10 m water depth reconstructed by the MAT from core GeoB2107-3 (Pereira et al., 2018) (brown line); SST derived from long-chain diol index (LDI) from core NAP 63–1 (Dauner et al., 2019) (green line); Mg/Ca-SST derived from *Globigerinoides ruber* from core 36GGC (Carlson et al., 2008) (light blue line). (d) Mg/Ca-SST derived from *Globigerinoides ruber* from core GeoB6211-2 (Chiessi et al., 2015) (dark blue line). The grey bar marks the Heinrich stadial 1 (18–15 ka BP). The latitude of each core located in the western Atlantic is shown in the graph. (For interpretation of the references to colour in this figure legend, the reader is referred to the web version of this article.)

areas confined to the continental shelf, a lack of sensitivity from MAT-SST estimations was observed (Lessa et al., 2014). Although Mg/Ca and TEX_{86} SST estimates showed large discrepancies in some subtropical regions (i.e. Weldeab et al. 2014), along the Brazilian coast the SST estimates from lipid-based biomarkers (TEX_{86} and/or LDI) exhibit similar patterns in relation to Mg/Ca-SST (Crivellari et al., 2019; Dauner et al., 2019). Discrepancy between Mg/Ca-SST and SST estimates from lipid-based biomarkers in the study areas was only observed for SSTs derived from $U^{k'}_{37}$, showing opposing patterns in comparison to Mg/Ca-SST (Crivellari et al., 2019; Dauner et al., 2019). This may be related to non-thermal physiological effects and/or to the fact that $U^{k'}_{37}$ represents subsurface temperature changes in the study areas (Crivellari et al., 2019; Dauner et al., 2019). The high temporal resolution records from the BC do not show a notable SST increase during HS1 (Carlson et al., 2008; Santos et al., 2017; Pereira et al., 2018; Fig. 3c), instead the SST responses appear to be muted, with such muted response being consistent between different proxies at the same latitude (Fig. 3c). Differently from Chiessi et al. (2015), the works from Carlson et al. (2008), Santos et al. (2017) and Pereira et al. (2018) analyzed cores from the central portion of the BC (Fig. 1). Thus, an additional explanation is required in order to reconcile the observed differences in SST responses during HS in the central BC domain compared to the NBC domain.

5.2. SACZ-SST feedback in the subtropical South Atlantic

Concomitantly with a reduced AMOC strength (McManus et al., 2004; Böhm et al., 2015; Henry et al., 2016), speleothem and marine records indicate a southward shift of the ITCZ (Wang et al., 2004; Mulitza et al., 2017) together with a strengthening of precipitation over eastern South America (Stríkis et al., 2015; Stríkis et al., 2018; Campos et al., 2019) during several HS (Fig. 4d-e). Lenters and Cook (1995) showed that enhanced precipitation in the SACZ is associated with low-level wind convergence maxima that are directly related to the interaction of the continental low with the South Atlantic high and the NE trade winds. During HS, the NE trade winds were stronger than the SE trades, as a response to a cooling of the Northern Hemisphere and a warming of the Southern Hemisphere (Broccoli et al., 2006; McGee et al., 2018). A southward displacement of the ITCZ occurs during HS because of such hemispherically thermal asymmetry. Thus, a strengthening of the SACZ during HS (Stríkis et al., 2015; Novello et al., 2017; Stríkis et al., 2018) can be explained by the intensification of the NE trade winds, which together with a southward displacement of the ITCZ caused an increase in the annual moisture flux into South America (Sifeddine et al., 2003; Wang et al., 2017). Since, most model simulations show a southward displacement of the ITCZ during AMOC slowdowns (Kageyama et al., 2013), it is plausible to consider that during those periods the SAMS/SACZ would strengthens due to increased moisture advection into South America. However, for the SAMS/SACZ area the results from model simulations are inconsistent (see Fig. 5 in Kageyama et al., 2013), with practically the same number of models showing increases or decreases in precipitation over the SAMS/SACZ.

A recent study from Campos et al. (2019) suggested that during HS austral summer precipitation only increased over eastern South America while the rest of tropical South America experienced precipitation increases during austral winter. Since this suggestion is based on precipitation anomalies from a model simulation and are not directly grounded on the spatial distribution of cloud bands from the Amazon southeastwards to the South Atlantic (defining the presence of SACZ) during HS, their findings do not conflict with our further interpretations. In addition, Campos et al. (2019) using a compilation of marine records showed that precipitation anomalies over drainage basins located in southeastern Brazil were probably not intense enough to produce increased fluvial discharge to the SE South American continental margin during HS. Thus, precipitation associated with the SACZ probably did not increase substantially during HS (Campos et al., 2019). However, cloud cover must have increased enough to produce an effect over SST. Nevertheless, our results together with the recent findings from Campos et al. (2019) highlight the need for a broad approach to explain South American HS hydroclimate.

Several studies focused on the understanding of the modern coupled variability of the SACZ and the underlying SST (Chaves and Nobre, 2004; De Almeida et al., 2007; Nobre et al., 2012; Jorgetti et al., 2014), but investigations of this ocean-atmosphere coupling during longer periods are still lacking. The absence of investigations regarding ocean-atmosphere processes related to the SACZ during the past millennial-scale events is probably due to the inability of climate models to represent the SAMS/SACZ in these periods. Mohtadi et al. (2016) highlights this issue by showing discrepancies between state-of-the-art model results (i.e. TraCE-21 k) and proxy data in the area of the SACZ during HS1. Therefore, it is reasonable to rely on modern model simulations and observational data in order to understand the processes driving SST changes in the subtropical South Atlantic, which is the approach that we have focus on in this study.

Jorgetti et al. (2014) demonstrated that positive SST anomalies in the subtropical South Atlantic are related to a southernmost position of the SACZ, although the strength of the SACZ is not determined by its geographical location (Carvalho et al., 2004). Chaves and Nobre (2004) showed that the SACZ strengthens when positive SST anomalies occur in the western South Atlantic. A subsequent increase in low clouds in the case of an oceanic SACZ (Carvalho et al., 2004) would diminish or reverse pre-existing positive SST anomalies, through the decrease of the incident shortwave solar radiation (Chaves and Nobre, 2004; De Almeida et al., 2007). This negative feedback mechanism suggests that cold SST anomalies that appear in model simulations (Chaves and Nobre, 2004; Nobre et al., 2012) synchronously with an intensified SACZ are generated due to the regional atmospheric response to warm anomalies. Thus, after the establishment of an intensified SACZ, the surface layer in the central part of the BC probably responded to the atmospheric forcing (SACZ-SST negative feedback). This caused a dampening of the initial warming, which explains the muted SST responses displayed between 20 and 30°S in the western South Atlantic. The absence of such feedback in the western equatorial Atlantic is probably related to different ocean-atmosphere dynamics and cloud type. The tropics have predominantly convective clouds and previous studies have shown that in the western equatorial Atlantic an increase in SST generates stronger convection and cloudiness, resulting in less longwave radiative heat loss from the surface and consequently reinforcing the positive SST anomaly (Wang and Enfield, 2001, 2003). On the other hand, in the subtropics the low clouds are predominant, which have minor effects on outgoing longwave radiation (OLR) but promote a decrease in incident shortwave solar radiation, cooling the underlying surface. These interpretations are corroborated by the analysis of instrumental data (Figs. S2 and S3), which shows the opposite relationship between OLR and SST in the tropics compared to the subtropics in the western South Atlantic.

Since foraminiferal-based SST estimations could include a seasonal bias (i.e. Fraile et al., 2009), one could also argue that since the SACZ is a summer atmospheric feature, foraminiferal-based SST proxies (i.e. Mg/Ca) would not be able to capture its signal. However, most of the SST records from the subtropical South Atlantic are derived from planktonic foraminifera assemblages and Mg/Ca from *G. ruber* (white). These proxies should be able to capture the SACZ-SST feedback signature, since the highest seasonal abundances of *G. ruber* (white) in the subtropical South Atlantic occur during austral summer (Venancio et al., 2017). Therefore, we suggest that such ocean-atmosphere interactions can explain why the positive SST response during HS is diminished in cores located under the oceanic sector of the SACZ (GL-1090 and 36GCC) compared to cores north (GeoB3129-1/3911–3; CDH-86, GeoB16202-2 and GL-1248) and south (GeoB6211-2) of this location (Figs. 1 and 3). The SACZ-SST feedback explains the different SST patterns during HS of cores GL-1090 in the central portion of the BC and GL-1248 in the NBC domain (Fig. 4b-c). The absence of abrupt warmings

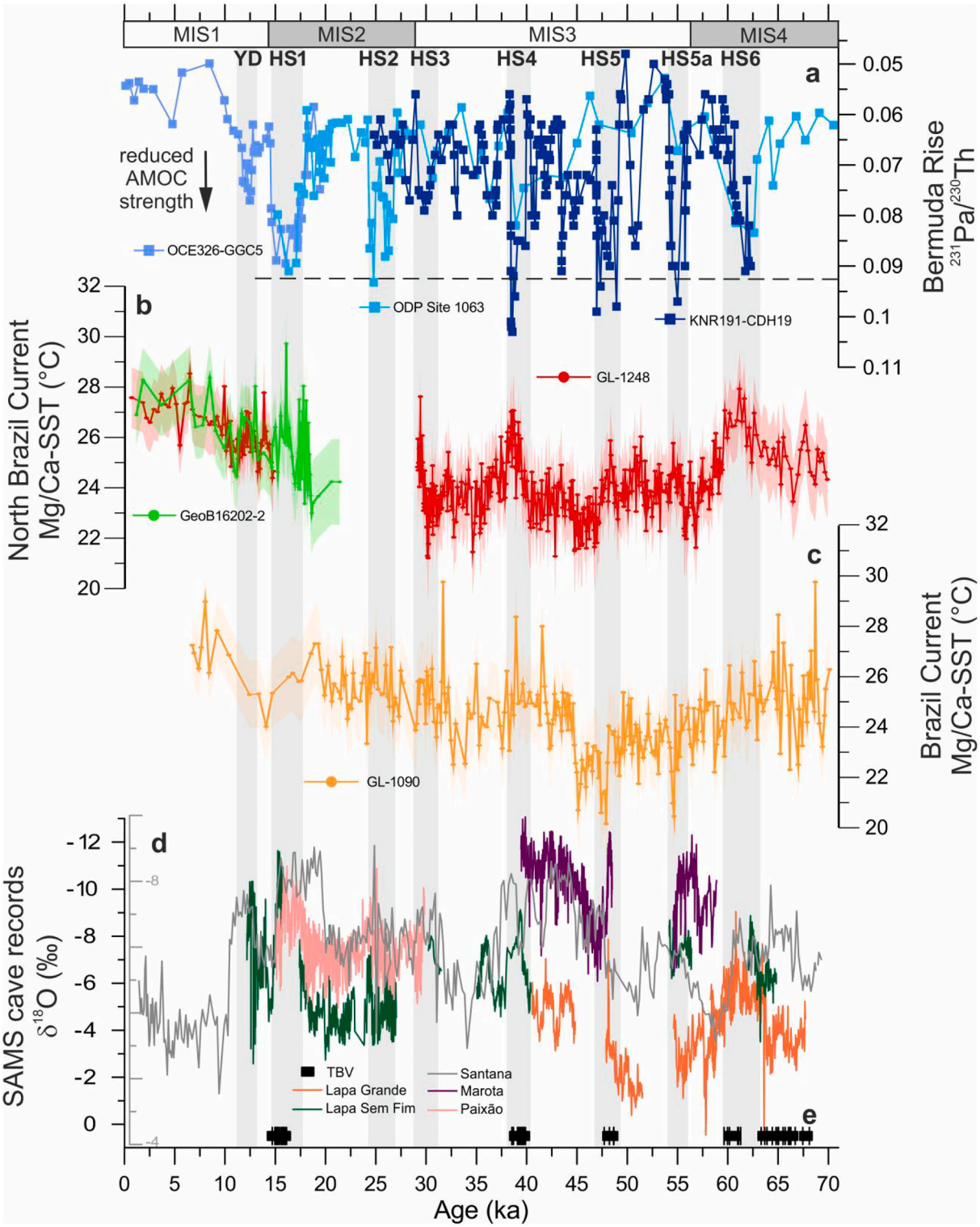

Fig. 4. Proxy records for the Atlantic and South America covering Heinrich stadials 6 to 1 (HS6-HS1), as well as the Younger Dryas (YD). (a) $^{231}Pa/^{230}Th$ records from Bermuda rise represented by blue lines and squares (OCE326-GGC5, McManus et al., 2004; ODP 1063, Böhm et al., 2015; KNR191-CDH19, Henry et al., 2016). The black dotted line marks the production ratio (0.093), which indicates sluggish overturning circulation. (b) Mg/Ca-SST of *G. ruber* (white) from cores GL-1248 (red line and dots) and GeoB16202-2 (light green line and dots) from the North Brazil Current domain, with their 2σ errors envelopes. (c) Mg/Ca-sea surface temperature (SST) of *Globigerinoides ruber* (white) from core GL-1090 (yellow line and dots) from the Brazil Current domain, with their 2σ errors envelopes. (d) $\delta^{18}O$ (‰) from speleothem records under the influence of the South American Monsoon System (SAMS) (Cruz et al., 2006; Stríkis et al., 2018). Caves Santana (grey line and y-axis), Lapa Grande (orange line), Lapa Sem Fim (dark green line), Marota (purple line) and Paixão (pink line). Please note that the y-axis is inverted. (e) Toca da Boa Vista (TBV) ^{230}Th ages of speleothem growth phases (black squares with error bars) in northeastern Brazil (Wang et al., 2004). Grey bars highlight the HS and the YD. Marine Isotope Stages (MIS) are delimited below the upper x-axis. (For interpretation of the references to colour in this figure legend, the reader is referred to the web version of this article.)

during all HS and the YD in core GL-1090 might be due to an intensified SACZ during these events, causing a dampening of the initial positive SST anomalies, which indicates that oceanic variations in the subtropical South Atlantic are a response to the atmospheric conditions associated with the SACZ.

6. Conclusions

SST reconstructions from the tropical and subtropical South Atlantic show disparate responses for HS6 to HS1. In the western equatorial Atlantic, abrupt warmings during HS are associated with reductions in cross-equatorial heat transport and boosted by regional ocean-atmosphere feedbacks linked to variations in the trade wind system. In the subtropical South Atlantic however, atmospheric forcing diminishes the positive SST response during HS by cutting off incoming shortwave solar radiation associated with to the increased cloud cover of the SACZ. The intensification of the SACZ during HS caused a dampening of the initial warming due to the SACZ-SST feedback. This exemplifies how regional feedback mechanism can cause a dampening of ocean surface warming initially triggered by the bipolar seesaw, locally masking the expression of the later phenomena on millennial timescales.

Supplementary data to this article can be found online at https://doi.org/10.1016/j.gloplacha.2020.103352.

Acknowledgments, samples, and data

We thank R. Kowsman (CENPES/ Petrobras) and Petrobras Core Repository staff (Macaé/Petrobras) for providing sediment core GL-1248 employed in this research. We thank S. Pape and M. Kölling for performing Mg/Ca analysis. CAPES financially supported I.M.V. with a scholarship (grant 88,887.156152/2017–00 and 88,881.161151/2017–01). M.H.S. would like to acknowledge FAPESP for the financial support (grant 2016/24014–9 and 2017–50,085-3). T.P.S. acknowledges the financial support from CAPES/PDSE (grant 99,999.007924/2014–03). B.B.D. appreciates the financial support from CAPES/FAPERJ (grant 202.134/2015). A.L.A. is a CNPq senior researcher (grant 306,385/2013–9) and thanks them for financial support (grant 99,999.002675/2015–03). C.M.C. acknowledges the financial support from FAPESP (grant 2018/15123–4), CAPES (grants 564/2015 and 88,881.313535/2019–01), CNPq (grants 302,607/2016–1 and 422,255/2016–5) and the Alexander von Humboldt Foundation. CNPq Project RAiN (grant 406,322/2018–0) supported this study. This study was also supported by CAPES-ASPECTO project (grant 88,887.091731/2014–01). This work was also funded through the DFG Research Center/Cluster of Excellence "The Ocean in the Earth System" and by the Helmholtz Climate Initiative REKLIM. The data reported in this paper will be archived in Pangaea (www.pangaea.de).

Declaration of Competing Interest

The authors declare that they have no known competing financial interests or personal relationships that could have appeared to influence the work reported in this paper.

References

Arz, H.W., Pätzold, J., Wefer, G., 1998. Correlated Millennial-Scale changes in Surface Hydrography and Terrigenous Sediment Yield Inferred from Last-Glacial Marine Deposits off Northeastern Brazil. Quat. Res. 50, 157–166. https://doi.org/10.1006/qres.1998.1992.

Barker, S., Greaves, M., Elderfield, H., 2003. A study of cleaning procedures used for foraminiferal Mg/Ca paleothermometry. Geochem. Geophys. Geosyst. 4, 1–20. https://doi.org/10.1029/2003GC000559".

Blaauw, M., 2010. Methods and code for "classical" age-modelling of radiocarbon sequences. Quaternary Geochronology 5 (5), 512–518. https://doi.org/10.1016/j.quageo.2010.01.002.

Blaauw, M., Christen, J.A., 2019. Flexible paleoclimate age–depth models using an autoregressive gamma process. Bayesian Anal. 6, 457–474. https://doi.org/10.1214/11-BA618.

Böhm, E., Lippold, J., Gutjahr, M., Frank, M., Blaser, P., Antz, B., Deininger, M., 2015. Strong and deep Atlantic meridional overturning circulation during the last glacial cycle. Nature 517 (7532), 73–76. https://doi.org/10.1038/nature14059.

Broccoli, A.J., Dahl, K.A., Stouffer, R.J., 2006. Response of the ITCZ to Northern Hemisphere cooling. Geophys. Res. Lett. L01702 https://doi.org/10.1029/2005GL024546.

Broecker, W.S., 1998. Paleocean circulation during the last deglaciation: a bipolar seesaw? Paleoceanography 13 (2), 119–121. https://doi.org/10.1029/97PA03707.

Caesar, L., Rahmstorf, S., Robinson, A., Feulner, G., Saba, V., 2018. Observed fingerprint of a weakening Atlantic Ocean overturning circulation. Nature. 556, 191–196. https://doi.org/10.1038/s41586-018-0006-5.

Campos, M.C., Chiessi, C.M., Prange, M., Mulitza, S., Kuhnert, H., Paul, A., Venancio, I. M., Albuquerque, A.L.S., Cruz, F.W., Bahr, A., 2019. A new mechanism for millennial scale positive precipitation anomalies over tropical South America. Quat. Sci. Rev. 225, 105990. https://doi.org/10.1016/j.quascirev.2019.105990.

Carlson, A.E., Oppo, D.W., Came, R.E., LeGrande, A.N., Keigwin, L.D., Curry, W.B., 2008. Subtropical Atlantic salinity variability and Atlantic meridional circulation during the last deglaciation. Geology 36 (12), 991–994. https://doi.org/10.1130/G25080A.1.

Carvalho, L.M.V., Jones, C., Liebmann, B., 2004. The South Atlantic Convergence Zone: Intensity, form, Persistence, and Relationships with Intraseasonal to Interannual activity and Extreme Rainfall. J. Clim. 17, 88–108. https://doi.org/10.1175/1520-0442(2004)017<0088:TSACZI>2.0.CO;2.

Chaves, R.R., Nobre, P., 2004. Interactions between sea surface temperature over the South Atlantic Ocean and the South Atlantic Convergence Zone. Geophys. Res. Lett. 31 (3), L03204 https://doi.org/10.1029/2003GL018647.

Chiessi, C.M., Mulitza, S., Mollenhauer, G., Silva, J.B., Groeneveld, J., Prange, M., 2015. Thermal evolution of the western South Atlantic and the adjacent continent during termination 1. Clim. Past 11 (6), 915–929. https://doi.org/10.5194/cp-11-915-2015.

Crivellari, S., Chiessi, C.M., Kuhnert, H., Häggi, C., da Costa Portilho-Ramos, R., Zeng, J.-Y., Zhang, Y., Schefuß, E., Mollenhauer, G., Hefter, J., Alexandre, F., Sampaio, G., Mulitza, S., 2018. Increased Amazon freshwater discharge during late Heinrich Stadial 1. Quat. Sci. Rev. 181, 144–155. https://doi.org/10.1016/j.quascirev.2017.12.005.

Crivellari, S., Chiessi, C.M., Kuhnert, H., Häggi, C., Mollenhauer, G., Hefter, J., Portilho-Ramos, R., Schefuß, E., Mulitza, S., 2019. Thermal response of the western tropical Atlantic to slowdown of the Atlantic Meridional Overturning Circulation. Earth Planet. Sci. Lett. 519, 120–129. https://doi.org/10.1016/j.epsl.2019.05.006.

Cruz, F., Burns, S.J., Karmann, I., Sharp, W., Vuille, M., Cardoso, A., Viana, O., 2005. Insolation-driven changes in atmospheric circulation over the past 116,000 years in subtropical Brazil. Nature 434, 63–65. https://doi.org/10.1029/2003JB002684.

Cruz, F.W., Burns, S.J., Karmann, I., Sharp, W.D., Vuille, M., 2006. Reconstruction of regional atmospheric circulation features during the late Pleistocene in subtropical Brazil from oxygen isotope composition of speleothems. Earth Planet. Sci. Lett. 248 (1–2), 494–506. https://doi.org/10.1016/j.epsl.2006.06.019.

Cruz, F.W., Vuille, M., Burns, S.J., Wang, X., Cheng, H., Werner, M., Nguyen, H., 2009. Orbitally driven east-west antiphasing of South American precipitation. Nature Geoscience 2 (3), 210–214. https://doi.org/10.1038/ngeo444.

da Portilho-Ramos, R.C., Ferreira, F., Calado, L., Frontalini, F., de Toledo, M.B., 2015. Variability of the upwelling system in the southeastern Brazilian margin for the last 110,000 years. Glob. Planet. Chang. 135, 179–189. https://doi.org/10.1016/j.gloplacha.2015.11.003.

Dauner, A.L.L., Mollenhauer, G., Bícego, M.C., de Souza, M.M., Nagai, R.H., Figueira, R. C.L., de Mahiques, M.M., de Sousa, S.H.M.E., Martins, C.C., 2019. Multi-proxy reconstruction of sea surface and subsurface temperatures in the western South Atlantic over the last ~75 kyr. Quat. Sci. Rev. 215, 22–34. https://doi.org/10.1016/j.quascirev.2019.04.020.

De Almeida, R.A.F., Nobre, P., Haarsma, R.J., Campos, E.J.D., 2007. Negative ocean-atmosphere feedback in the South Atlantic Convergence Zone. Geophys. Res. Lett. 34 (18) https://doi.org/10.1029/2007GL030401.

Deplazes, G., Lückge, A., Peterson, L.C., Timmermann, A., Hamann, Y., Hughen, K.A., Haug, G.H., 2013. Links between tropical rainfall and North Atlantic climate during the last glacial period. Nature Geoscience 6 (2), 1–5. https://doi.org/10.1038/ngeo1712.

Drijfhout, S.S., Weber, S.L., van der Swaluw, E., 2011. The stability of the MOC as diagnosed from model projections for pre-industrial, present and future climates. Clim. Dyn. 37 (7), 1575–1586. https://doi.org/10.1007/s00382-010-0930-z.

EPICA Community Members, 2006. One-to-one coupling of glacial climate variability in Greenland and Antarctica. Nature 444, 195–198. https://doi.org/10.1038/nature05301.

Fraile, I., Mulitza, S., Schulz, M., 2009. Modeling planktonic foraminiferal seasonality: Implications for sea-surface temperature reconstructions. Mar. Micropaleontol. 72, 1–9. https://doi.org/10.1016/j.marmicro.2009.01.003.

Gray, W.R., Evans, D., 2019. Nonthermal Influences on Mg/ca in Planktonic Foraminifera: a Review of Culture Studies and Application to the last Glacial Maximum. Paleoceanogr. Paleoclimatol. 34, 306–315. https://doi.org/10.1029/2018PA003517.

Groeneveld, J., Chiessi, C.M., 2011. Mg/ca of Globorotalia inflata as a recorder of permanent thermocline temperatures in the South Atlantic. Paleoceanography 26. https://doi.org/10.1029/2010PA001940.

Hastenrath, S., 2012. Exploring the climate problems of Brazil's Nordeste: a review. Clim. Chang. 112 (2), 243–251. https://doi.org/10.1007/s10584-011-0227-1.

Hastenrath, S., Merle, J., 1987. Annual cycle of subsurface thermal structure in the tropical Atlantic Ocean. J. Phys. Oceanogr. 17, 1518–1538.

Henry, L.G., McManus, J.F., Curry, W.B., Roberts, N.L., Piotrowski, A.M., Keigwin, L.D., 2016. North Atlantic Ocean circulation and abrupt climate change during the last glaciation. Science 353 (6298), 470–474. https://doi.org/10.1126/science.aaf5529.

Jennerjahn, T.C., Ittekkot, V., Arz, H.W., Behling, H., Pätzold, J., Wefer, G., 2004. Asynchronous Terrestrial and Marine Signals of climate Change during Heinrich events. Science (80-.) 306. https://doi.org/10.1126/science.1102490, 2236 LP – 2239.

Jorgetti, T., da Silva Dias, P.L., de Freitas, E.D., 2014. The relationship between South Atlantic SST and SACZ intensity and positioning. Clim. Dyn. 42, 3077–3086. https://doi.org/10.1007/s00382-013-1998-z.

Kageyama, M., Merkel, U., Otto-Bliesner, B., Prange, M., Abe-Ouchi, A., Lohmann, G., Ohgaito, R., Roche, D.M., Singarayer, J., Swingedouw, D., Zhang, X., 2013. Climatic impacts of fresh water hosing under last Glacial Maximum conditions: a multi-model study. Clim. Past 9, 935–953. https://doi.org/10.5194/cp-9-935-2013.

Lenters, J.D., Cook, K.H., 1995. Simulation and Diagnosis of the Regional Summertime Precipitation Climatology of South America. J. Clim. 8, 2988–3005. https://doi.org/10.1175/1520-0442(1995)008<2988:SADOTR>2.0.CO;2.

Lessa, D.V., Ramos, R.P., Barbosa, C.F., da Silva, A.R., Belem, A., Turcq, B., Albuquerque, A.L., 2014. Planktonic foraminifera in the sediment of a western boundary upwelling system off Cabo Frio, Brazil. Mar. Micropaleontol. 106, 55–68. https://doi.org/10.1016/j.marmicro.2013.12.003.

Lessa, D.V.O., Santos, T.P., Venancio, I.M., Albuquerque, A.L.S., 2017. Offshore expansion of the Brazilian coastal upwelling zones during Marine Isotope Stage 5. Glob. Planet. Chang. 158 https://doi.org/10.1016/j.gloplacha.2017.09.006.

Lessa, D.V.O., Santos, T.P., Venancio, I.M., Santarosa, A.C.A., dos Santos Junior, E.C., Toledo, F.A.L., Costa, K.B., Albuquerque, A.L.S., 2019. Eccentricity-induced expansions of Brazilian coastal upwelling zones. Glob. Planet. Chang. 179, 33–42. https://doi.org/10.1016/j.gloplacha.2019.05.002.

Liu, W., Xie, S.-P., Liu, Z., Zhu, J., 2017. Overlooked possibility of a collapsed Atlantic Meridional Overturning Circulation in warming climate. Sci. Adv. 3, e1601666 https://doi.org/10.1126/sciadv.1601666.

Locarnini, R.A., Mishonov, A.V., Baranova, O.K., Boyer, T.P., Zweng, M.M., Garcia, H.E., Reagan, J.R., Seidov, D., Weathers, K., Paver, C.R., Smolyar, I., 2018. World Ocean Atlas 2018, volume 1: Temperature. A. Mishonov Technical Ed.; NOAA Atlas NESDIS, 81, p. 52.

Matano, R.P., Schlax, M.G., Chelton, D.B., 1993. Seasonal variability in the southwestern Atlantic. J. Geophys. Res. Ocean. 98, 18027–18035. https://doi.org/10.1029/93JC01602.

McGee, D., Moreno-Chamarro, E., Green, B., Marshall, J., Galbraith, E., Bradtmiller, L., 2018. Hemispherically asymmetric trade wind changes as signatures of past ITCZ shifts. Quat. Sci. Rev. 180, 214–228. https://doi.org/10.1016/j.quascirev.2017.11.020.

McManus, J.F., Francois, R., Gherardi, J.-M., Keigwin, L.D., Brown-Leger, S., 2004. Collapse and rapid resumption of Atlantic meridional circulation linked to deglacial climate changes. Nature 428 (6985), 834–837. https://doi.org/10.1038/nature02494.

Mix, A.C., Ruddiman, W.F., McIntyre, A., 1986. Late Quaternary paleoceanography of the Tropical Atlantic, 1: Spatial variability of annual mean sea-surface temperatures, 0-20,000 years B.P. Paleoceanography 1, 43–66. https://doi.org/10.1029/PA001i001p00043.

Mohtadi, M., Prange, M., Steinke, S., 2016. Palaeoclimatic insights into forcing and response of monsoon rainfall. Nature 533, 191–199. https://doi.org/10.1038/nature17450.

Mulitza, S., Chiessi, C.M., Cruz, A.P.S., Frederichs, T.W., Gomes, J.G., Gurgel, M.H.C., Haberkern, J., Huang, E., Jovane, L., Kuhnert, H., Pittauerova, D., Reiners, S.J., Roud, S.C., Schefuß, E., et al., 2013. Response of Amazon Sedimentation to Deforestation, Land Use and Climate Variability. Cruise No. MSM20/3 (February 19 March 11, 2012). In: Recife (Brazil) Bridgetown (Barbados). MARIA S. MERIAN berichte, MSM20/3. DFG Senatskommission für Ozeanographie.

Mulitza, S., Chiessi, C.M., Schefuß, E., Lippold, J., Wichmann, D., Antz, B., Zhang, Y., 2017. Synchronous and proportional deglacial changes in Atlantic meridional overturning and northeast Brazilian precipitation. Paleoceanography 32 (6), 622–633. https://doi.org/10.1002/2017PA003084.

Nace, T.E., Baker, P.A., Dwyer, G.S., Silva, C.G., Rigsby, C.A., Burns, S.J., Zhu, J., 2014. The role of North Brazil Current transport in the paleoclimate of the Brazilian Nordeste margin and paleoceanography of the western tropical Atlantic during the late Quaternary. Palaeogeography, Palaeoclimatology, Palaeoecology 415, 3–13. https://doi.org/10.1016/j.palaeo.2014.05.030c.

Nobre, P., De Almeida, R.A., Malagutti, M., Giarolla, E., 2012. Coupled ocean-atmosphere variations over the South Atlantic Ocean. J. Clim. 25 (18), 6349–6358. https://doi.org/10.1175/JCLI-D-11-00444.1.

North Greenland Ice Core Project members, 2004. High-resolution record of Northern Hemisphere climate extending into the last interglacial period. Nature 431 (7005), 147–151. https://doi.org/10.1038/nature02805.

Novello, V.F., Cruz, F.W., Vuille, M., Stríkis, N.M., Edwards, R.L., Cheng, H., Santos, R.V., 2017. A high-resolution history of the South American Monsoon from Last Glacial Maximum to the Holocene. Scientific Reports 7, 1–8. https://doi.org/10.1038/srep44267.

Parker, A., 2016. Atlantic Meridional Overturning Circulation is stable under global warming. Proc. Natl. Acad. Sci. 113 https://doi.org/10.1073/pnas.1604187113. E2760 LP-E2761.

Pereira, L.S., Arz, H.W., Pätzold, J., Portilho-Ramos, R.C., 2018. Productivity Evolution in the South Brazilian Bight during the last 40,000 years. Paleoceanogr. Paleoclimatol. 33, 1339–1356. https://doi.org/10.1029/2018PA003406.

Peterson, R.G., Stramma, L., 1991. Upper-level circulation in the South Atlantic Ocean. Prog. Oceanogr. 26 (1), 1–73. https://doi.org/10.1016/0079-6611(91)90006-8.

Rodrigues, R.R., Rothstein, L.M., Wimbush, M., 2007. Seasonal Variability of the South Equatorial Current Bifurcation in the Atlantic Ocean: a Numerical Study. J. Phys. Oceanogr. 37 (1), 16–30. https://doi.org/10.1175/JPO2983.1.

Santos, T.P., Lessa, D.O., Venancio, I.M., Chiessi, C.M., Mulitza, S., Kuhnert, H., Govin, A., Machado, T., Costa, K.B., Toledo, F., Dias, B.B., Albuquerque, A.L.S., 2017. Prolonged warming of the Brazil current precedes deglaciations. Earth Planet. Sci. Lett. 463, 1–12. https://doi.org/10.1016/j.epsl.2017.01.014.

Shakun, J.D., Clark, P.U., He, F., Marcott, S.A., Mix, A.C., Liu, Z., Otto-Bliesner, B., Schmittner, A., Bard, E., 2012. Global warming preceded by increasing carbon dioxide concentrations during the last deglaciation. Nature 484, 49–54. https://doi.org/10.1038/nature10915.

Sifeddine, A., Spadano Albuquerque, A.L., Ledru, M.P., Turcq, B., Knoppers, B., Martin, L., Bittencourt, A.C.D.S.P., 2003. A 21 000 cal years paleoclimatic record from Caçó Lake, northern Brazil: Evidence from sedimentary and pollen analyses. Palaeogeography, Palaeoclimatology, Palaeoecology 189 (1–2), 25–34. https://doi.org/10.1016/S0031-0182(02)00591-6.

Stocker, T.F., Johnsen, S.J., 2003. A minimum thermodynamic model for the bipolar seesaw. Paleoceanography 18 (4), 1–9. https://doi.org/10.1029/2003PA000920.

Stramma, L., England, M., 1999. On the water masses and mean circulation of the South Atlantic Ocean. J. Geophys. Res. 104 (C9), 20863. https://doi.org/10.1029/1999JC900139.

Stramma, L., Fischer, J., Reppin, J., 1995. The North Brazil Undercurrent. Deep-Sea Res. I Oceanogr. Res. Pap. 42 (5), 773–795. https://doi.org/10.1016/0967-0637(95)00014-W.

Stríkis, N.M., Chiessi, C.M., Cruz, F.W., Vuille, M., Cheng, H., De Souza Barreto, E.A., Sales, H.D.R., 2015. Timing and structure of Mega-SACZ events during Heinrich Stadial 1. Geophysical Research Letters 42 (13), 5477–5484. https://doi.org/10.1002/2015GL064048.

Stríkis, N.M., Cruz, F.W., Barreto, E.A.S., Naughton, F., Vuille, M., Cheng, H., Sales, H.R., 2018. South American monsoon response to iceberg discharge in the North Atlantic. Proc. Natl. Acad. Sci. 201717784. https://doi.org/10.1073/pnas.1717784115.

Vahlenkamp, M., 2013. The Anatomy of Heinrich Event 1 – A Multiproxy Study of Centennial to Millennial Scale Climate Change off Brazil. Master's Thesis. University of Bremen, p. 70.

Venancio, I., Belem, A., Santos, T., Lessa, D., Albuquerque, A., Mulitza, S., Kucera, M., 2017. Calcification depths of planktonic foraminifera from the southwestern Atlantic derived from oxygen isotope analyses of sediment trap material. Marine Micropaleontology 136 (August), 37–50. https://doi.org/10.1016/j.marmicro.2017.08.006.

Venancio, I.M., Mulitza, S., Govin, A., Santos, T.P., Lessa, D.O., Albuquerque, A.L.S., et al., 2018. Millennial- to orbital-scale responses of western equatorial Atlantic thermocline depth to changes in the trade wind system since the last Interglacial. Paleoceanogr. Paleoclimatol. 33 https://doi.org/10.1029/2018PA003437.

Wang, C., Enfield, D.B., 2001. The Tropical Western Hemisphere warm Pool. Geophys. Res. Lett. 28, 1635–1638. https://doi.org/10.1029/2000GL011763.

Wang, C., Enfield, D.B., 2003. A further Study of the Tropical Western Hemisphere warm Pool. J. Clim. 16, 1476–1493. https://doi.org/10.1175/1520-0442-16.10.1476.

Wang, X., Auler, A.S., Edwards, R.L., Cheng, H., Cristalli, P.S., Smart, P.L., Shen, C.-C., 2004. Wet periods in northeastern Brazil over the past 210 kyr linked to distant climate anomalies. Nature 432 (7018), 740–743. https://doi.org/10.1038/nature03067.

Wang, X., Edwards, R.L., Auler, A.S., Cheng, H., Kong, X., Wang, Y., Chiang, H.W., 2017. Hydroclimate changes across the Amazon lowlands over the past 45,000 years. Nature 541 (7636), 204–207. https://doi.org/10.1038/nature20787.

Weldeab, S., Lea, D.W., Oberhänsli, H., Schneider, R.R., 2014. Links between southwestern tropical Indian Ocean SST and precipitation over southeastern Africa over the last 17kyr. Palaeogeogr. Palaeoclimatol. Palaeoecol. 410, 200–212. https://doi.org/10.1016/j.palaeo.2014.06.001.

Weldeab, S., Schneider, R.R., Kölling, M., 2006. Deglacial Sea surface temperature and salinity increase in the western tropical Atlantic in synchrony with high latitude climate instabilities. Earth Planet. Sci. Lett. 241 (3–4), 699–706. https://doi.org/10.1016/j.epsl.2005.11.012.

Wolff, E.W., Chappellaz, J., Blunier, T., Rasmussen, S.O., Svensson, A., 2010. Millennial-scale variability during the last glacial: the ice core record. Quat. Sci. Rev. 29 (21−22), 2828–2838. https://doi.org/10.1016/j.quascirev.2009.10.013.

Xie, P., Arkin, P.A., 1997. Global recipitation: a 17-year monthly analysis based on gauge observations, satellite estimates, and numerical model outputs. Bull. Am. Meteorol. Soc. 78, 2539–2558. https://doi.org/10.1175/1520-0477(1997)078<2539:GPAYMA>2.0.CO;2.

Zhang, Y., Chiessi, C.M., Mulitza, S., Sawakuchi, A.O., Häggi, C., Zabel, M., Portilho-Ramos, R.C., Schefuß, E., Crivellari, S., Wefer, G., 2017. Different precipitation patterns across tropical South America during Heinrich and Dansgaard-Oeschger stadials. Quat. Sci. Rev. 177, 1–9. https://doi.org/10.1016/j.quascirev.2017.10.012.